A new interaction potential for swarming models

J. A. Carrillo[a], S. Martin[*,b], V. Panferov[c]

[a] *ICREA and Departament de Matemàtiques, Universitat Autònoma de Barcelona, E-08193 Bellaterra, Spain.*
[b] *Department of Mathematics, Technische Universität Kaiserslautern, Erwin-Schrödinger-Straße, 67663 Kaiserslautern, Germany. Phone: (+49)-(0)-631-2054491, Fax: (+49)-(0)-631-2054986*
[c] *Department of Mathematics, California State University Northridge Northridge, CA 91330-8313, USA*

Abstract

We consider a self-propelled particle system which has been used to describe certain types of collective motion of animals, such as fish schools and bird flocks. Interactions between particles are specified by means of a pairwise potential, repulsive at short ranges and attractive at longer ranges. The exponentially decaying Morse potential is a typical choice, and is known to reproduce certain types of collective motion observed in nature, particularly aligned flocks and rotating mills. We introduce a class of interaction potentials, that we call Quasi-Morse, for which flock and rotating mills states are also observed numerically, however in that case the corresponding macroscopic equations allow for explicit solutions in terms of special functions, with coefficients that can be obtained numerically without solving the particle evolution. We compare thus obtained solutions with long-time dynamics of the particle systems and find a close agreement for several types of flock and mill solutions.

Key words: swarming patterns, individual based models, self-propelled interacting particles, quasi-Morse potentials
2010 MSC: 92D50, 82C22, 92C15, 65K05

1. Introduction

Emerging behaviors in interacting particle systems have received a lot of attention in research in recent years. Topics range from diverse fields of applications such as animal collective behavior, traffic, crowd dynamics and crystallization. Self-organization in the absence of leaders has been reported in several

[*] Corresponding author
Email addresses: carrillo@mat.uab.es (J. A. Carrillo), smartin@mathematik.uni-kl.de (S. Martin), vladislav.panferov@csun.edu (V. Panferov)
[a] *On leave from:* Department of Mathematics, Imperial College London, London SW7 2AZ, UK.

species which coordinate their movement (swarming), and several models have been proposed for their explanation [37, 35, 7, 9, 17, 18].

Many of these models are based on zones in which at least 3 basic effects are included: short-range repulsion, long-range attraction and alignment. Despite of the fact that some recent works [2] defend that the most important interaction of individuals is with their nearest neighbors independently how far they are, most of the models for swarming acquire this 3-zone basic scheme. These kind of models have been very popular for modeling fish schools [30, 31, 28, 3, 4], starlings [29] or ducks [33, 34]. Mathematicians have started in recent years to attack one of the most striking features of these *simple looking* models: the diversity of swarming states, also called patterns in the biology community, their emergence and stability.

The individual level description of these phenomena leads to certain particle systems, called Individual Based Models (IBMs), with some common aspects. Typically, the attraction-repulsion is modeled through pairwise effective potentials depending on the distance between individuals. An asymptotic speed for particles is imposed either by working in the constrained set of a sphere in velocity space [40, 25, 19] or by adding a term of balance between self-propulsion and friction which effectively fixes the speed to a limiting value for large times [32, 21]. In this work, we will not include any alignment mechanism. We refer to [13] for a survey on results related to kinetic modeling in swarming.

In section 2 we will review some of these IBMs, and discuss the appearance of two main swarming patterns: mills and flocks. These patterns are easily observed in particle simulations [21, 11] and reported in detail for certain particular potentials, the so-called Morse potentials. We will give a precise definition of flocks and mills as solutions of the kinetic equation associated to the particle systems also in Section 2. Section 3 introduces Quasi-Morse potentials as fundamental solutions of certain linear PDEs. This structure of the Quasi-Morse potentials allows us to express the flock and mill solutions in terms of basis functions associated to these PDEs. We will show that the Quasi-Morse potentials are biologically relevant in essentially the same parameter range as the Morse potentials. Finally, Section 4 is devoted to propose an algorithm to compute the scalar coefficients in the expansion of the flock and mill patterns in terms of the basis functions associated with the Quasi-Morse PDE operators. The strategy uses ideas of constrained optimization methods. We finally compare the results for flocks in 2D and 3D and mills in 2D to particle simulations showing a good agreement, even for moderate number of particles. As a conclusion, we demonstrate that the proposed Quasi-Morse potentials are a very good alternative to Morse potentials as they share many of their features, and at the same time enable explicit computation of the macroscopic density profiles.

2. Swarming: Models & Patterns

We will consider a simple second order model for swarming analyzed in [21] consisting of the attraction-repulsion of N interacting self-propelled particles located at $x_i \in \mathbb{R}^n$ with velocities $v_i \in \mathbb{R}^n$ in a host medium with friction,

with $n = 1, 2, 3$. Friction is modeled by Rayleigh's law and as a result, an asymptotic speed for the individuals is fixed by the compensation of friction and self-propulsion. More precisely, the time evolution is governed by the equations of motion

$$\begin{aligned} \frac{dx_i}{dt} &= v_i \,, \\ \frac{dv_i}{dt} &= \alpha v_i - \beta v_i |v_i|^2 - \nabla_{x_i} \sum_{i \neq j} W(x_i - x_j) \,, \end{aligned} \tag{1}$$

where W is a pairwise interaction potential and α, β are effective values for propulsion and friction forces, see [32, 21, 16, 15] for more discussion. The interaction potential $W : \mathbb{R}^n \times \mathbb{R}^n \to \mathbb{R}$ is assumed to be radially symmetric: $W(x) = U(|x|)$, $x \in \mathbb{R}^n$. The typical asymptotic speed of the individuals is $\sqrt{\alpha/\beta}$. The Morse potential is defined by taking

$$U(r) = -C_A e^{-r/l_A} + C_R e^{-r/l_R},$$

where C_A, C_R are the attractive and repulsive strengths, and l_A, l_R are their respective length scales. We set $V(r) = -\exp(-r/l_A)$, $C = C_R/C_A$, and $l = l_R/l_A$ to obtain

$$U(r) = C_A \left[V(r) - CV\left(\frac{r}{l}\right) \right].$$

The choice of this potential is motivated in [21] for being one of the simplest choices of integrable potentials with easily computable conditions to distinguish the relevant parameters in biological swarms. In fact, it is straightforward to check that in the range $C > 1$ and $l < 1$ the potential $U(r)$ is short-range repulsive and long-range attractive with a unique minimum defining a typical distance between particles. Moreover, in this regime the sign of the integral of the potential:

$$\mathcal{U} := \int_0^\infty W(x)\, dx = \mathcal{V}(1 - Cl^n) \qquad \text{with } \mathcal{V} := \int_0^\infty V(r) r^{n-1}\, dr < 0 \,, \tag{2}$$

gives a criterion to distinguish between the so-called H-stable and catastrophic regimes. This condition reads as $Cl^n - 1 < 0$ for the catastrophic case in any dimension n, see [21, 38]. This property of the potential is important since it is related to the typical patterns emerging in such systems, as classified in [21].

Flocks, where particles tend to form groups, moving with the same velocity, and milling solutions, where rotatory states are formed are of particular interest and are observed in particle and hydrodynamic simulations [21, 14] in $n = 2$. Actually, they typically emerge in the large time behavior of the system of particles (1) in the catastrophic regime $Cl^2 < 1$ with $C > 1$ and $l < 1$. In the same range of parameters, randomly chosen initial data lead also to other patterns such as double mills and flocks [21, 12]. However mills are not observed in the H-stable regime $Cl^2 > 1$ with $C > 1$ and $l < 1$ while flocks do.

Assuming the weak coupling scaling [20, 36, 8, 39] in which the range of interaction is kept fixed and the strength of interaction is divided proportionally between particles, we pass to the rescaled formulation:

$$\begin{aligned}\frac{dx_i}{dt} &= v_i\,,\\ \frac{dx_i}{dt} &= v_i(\alpha-\beta|v_i|^2) - \frac{1}{N}\nabla_{x_i}\sum_{i\neq j}U(|x_i-x_j|)\,.\end{aligned}$$

This system has a well-defined limit as $N\to\infty$ which can be expressed as a solution of the corresponding mean-field equation:

$$\partial_t f + v\cdot\nabla_x f + F[\rho]\cdot\nabla_v f + \operatorname{div}\left(\left(\alpha-\beta|v|^2\right)vf\right) = 0\,, \tag{3}$$

with

$$\rho(t,x) := \int f(t,x,v)\mathrm{d}v\,.$$

Here, $f(t,x,v):\mathbb{R}\times\mathbb{R}^n\times\mathbb{R}^n\to\mathbb{R}$ is the phase-space density, and $\rho(t,x)$ is the averaged (macroscopic) density. The mean-field interaction is given by $F[\rho]=-\nabla_x W\star\rho$.

The limit $N\to\infty$ has been established rigorously for smooth potentials $W\in C_b^2$ in [20, 36, 8, 39], in [10, 6] for more general models with and without noise, and for more general potentials, with possibly singular behavior at zero, including the Morse potential (2) in the recent result [27].

2.1. Flock and Mill States

We are interested in computing certain relevant particular solutions of the Vlasov-like equation for swarming in (3). In fact, we can formally find monokinetic solutions of (3) by inserting the ansatz:

$$f(t,x,v) = \rho(t,x)\,\delta(v-u(t,x)),$$

in the weak formulation of (3). The result in [16, 12] is that ρ and u should satisfy the following set of hydrodynamic equations:

$$\begin{cases}\dfrac{\partial\rho}{\partial t} + \operatorname{div}_x(\rho u) = 0,\\[2ex] \rho\,\dfrac{\partial u}{\partial t} + \rho\,(u\cdot\nabla_x)u = \rho\,(\alpha-\beta|u|^2)u - \rho\,(\nabla_x W\star\rho).\end{cases} \tag{4}$$

Definition 1. *A* flock *is a solution f_F of (3) of the form:*

$$f_F(t,x,v) = \rho_F(x-tu_0)\,\delta(v-u_0)\,,\ |u_0| = \sqrt{\frac{\alpha}{\beta}}\,,$$

with $u_0\in\mathbb{R}^n$ and ρ_F a probability measure in $\mathbb{R}^n$.

Obviously, flock solutions are determined by their density profile ρ_F and have the structure of traveling waves in the direction of the velocity vector u_0. It is straightforward to see that the density of a flock is characterized by the following equation:

Proposition 1. *The function $f_F \geq 0$ is a flock solution if and only if the macroscopic density ρ_F satisfies*

$$\nabla_x W \star \rho_F = 0 \quad \text{on the support of } \rho_F \,. \tag{5}$$

There are singular solutions to (5) obtained by concentrating all the mass uniformly in a suitable sphere, the so-called Delta rings [12], whose stability for first order models has recently been studied in [1] for certain potentials. Also, there are solutions to (5) given by smooth compactly supported densities for combination of suitable powers in 1D [22, 23], for the Morse potential in 1D [5], and for combination of powers when one of them is the repulsive Newtonian potential [24] in 2D. In fact, the set of solutions to (5) can be very complicated even in one dimension [22, 23, 26] depending on the regularity of the potential.

Let us remark that since we assume the radial symmetry of the potential, one expects that the density of the flocking solutions to (5) is radially symmetric as well and that it is supported in a ball $B(0, R_F)$ with $R_F > 0$. This is reinforced by the fact that the convolution of radial functions is radial, see below for more precise statements. We will reduce ourselves to find flocking solutions with radial symmetry in the rest of this paper, that is, densities $\rho_F(|x|)$ satisfying

$$W \star \rho_F = C \quad \text{in } B(0, R_F)\,,$$

for some constant $C \in \mathbb{R}$.

Another interesting type of solutions that spontaneously show up in particle simulations are *mills*, they correspond to motion with the velocity field of a point vortex:

$$u_M = \pm \sqrt{\frac{\alpha}{\beta}}\, \frac{x^\perp}{|x|}\,, \tag{6}$$

where $x = (x_1, x_2)$, $x^\perp = (-x_2, x_1)$, such that $\rho_M(|x|)$ is a radially symmetric stationary solution to (4).

Definition 2. *A* mill *is a solution f_M of (3) of the form:*

$$f_M(t, x, v) = \rho_M(x)\, \delta(v - u_M)\,,$$

with u_M given by (6) and ρ_M radially symmetric.

As shown in [32, 12, 14], mill solutions can also be characterized as:

Proposition 2. *$\rho_M(x)$ is a mill density if an only if*

$$\nabla \left[W \star \rho - \frac{\alpha}{\beta} \log |x| \right] = 0, \qquad \text{on the support of } \rho\,.$$

As discussed above, one can obtain singular mill solutions by concentrating all particles in a ring [12]. However, we will search for radial solutions supported in an annulus $B(R_m, R_M)$ with $0 < R_m < R_M$, and therefore, mill radial solutions supported in $B(R_m, R_M)$ are characterized by

$$W \star \rho_M = D + \frac{\alpha}{\beta} \log |x| \quad \text{in } B(R_m, R_M)\,, \tag{7}$$

for some constant $D \in \mathbb{R}$.

2.2. Convolution of radial functions

Given a density $\bar{\rho}(|x|)$, then the convolution term rewrites:

$$(W \star \bar{\rho})(x) = \int_{\mathbb{R}^n} W(x-y)\bar{\rho}(|y|)\mathrm{d}y = \int_0^\infty \int_{\partial B(0,1)} W(x - s\omega)\bar{\rho}(s)s^{n-1}\mathrm{d}\omega\mathrm{d}s$$

which is *not* a convolution in $r = |x|$ anymore, but rather is given by an operator of the following form:

$$(W \star \bar{\rho})(r) = \int_{\mathbb{R}^+} \Psi(r,s)\bar{\rho}(s)\mathrm{d}s$$

with

$$\Psi(r,s) = s^{n-1} \int_{\partial B(0,1)} U(|re_1 - s\omega|)\mathrm{d}\omega\,.$$

Expressing it in polar ($n = 2$) or spherical ($n = 3$) coordinates, we get the functions

$$\Psi(r,s) = s \int_0^{2\pi} U\left(\sqrt{r^2 - 2rs\cos\theta + s^2}\right)\mathrm{d}\theta \tag{8}$$

for $n = 2$ and

$$\begin{aligned}\Psi(r,s) &= s^2 \int_0^{2\pi}\int_0^{\pi} U(|re_1 - s\omega(\theta,\nu)|)\,\sin\nu\,\mathrm{d}\nu\,\mathrm{d}\theta \\ &= 2\pi s^2 \int_0^{\pi} U\left(\sqrt{r^2 - 2rs\cos\nu + s^2}\right)\,\sin\nu\,\mathrm{d}\nu\,,\end{aligned} \tag{9}$$

with $\omega(\theta,\nu) = (\cos\nu, \sin\nu\cos\theta, \sin\nu\sin\theta)$ for $n = 3$.

3. Quasi-Morse potentials and their explicit solvability

In this section, we define Quasi-Morse potentials for $n = 1, 2, 3$ and discuss their properties. These Quasi-Morse potentials will yield biologically relevant shapes similar to the Morse potentials, and we show that flock and mill solutions can be computed explicitly up to constants.

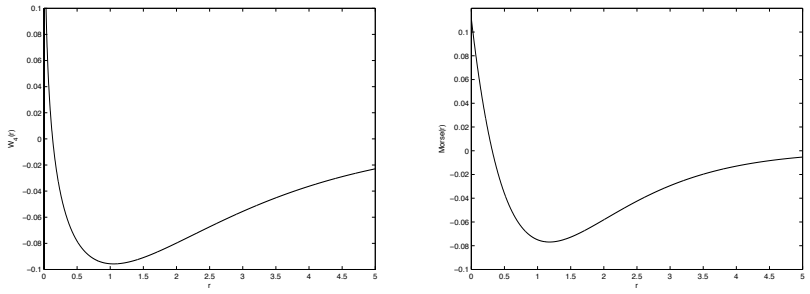

(a) Quasi-Morse potential (b) Morse potential

Figure 1: Comparison of potentials: Both yield the biologically relevant shape of short-range repulsion and long-range attraction (Quasi-Morse: $n = 2, C = \frac{10}{9}, l = 0.75, k = \frac{1}{2}, \lambda = 4$, Morse: $C = \frac{10}{9}, l = 0.75, k = 1, \lambda = 2$).

3.1. Definition and comparison

Definition 3. *Let $V : \mathbb{R}^+ \to \mathbb{R}$ denote the radially symmetric solution of the n-dimensional* screened Poisson equation $\Delta u - k^2 u = \delta_0$*, for a given $k > 0$, that vanishes at infinity. Let $C, l, \lambda \in \mathbb{R}$ be further positive parameters. Then we say that $U(|x|)$ is the n-*dimensional Quasi-Morse potential *if*

$$U(r) := \lambda \left(V(r) - C\, V\left(\frac{r}{l}\right) \right) .$$

Using the radially symmetric ansatz, the screened Poisson equation reduces to a second-order ordinary differential equation dependent on the space dimension. For relevant $n = 1, 2, 3$ this ODE possesses two linearly independent solutions. We therefore have

Corollary 1. *Quasi-Morse potentials for $n = 1, 2, 3$ are well-defined and constructed from the following fundamental solution:*

$$\begin{cases} n = 1: & V(r) = -\frac{1}{2k} e^{-kr} \\ n = 2: & V(r) = -\frac{1}{2\pi} K_0(kr) \\ n = 3: & V(r) = -\frac{1}{4\pi} \frac{e^{-kr}}{r} \end{cases}$$

where K_0 is the modified Bessel function of second kind. For $n = 1$, the Quasi-Morse potential equals the Morse potential.

We illustrate the Quasi-Morse potential in comparison to the Morse potential for $n = 2$ with parameters $C = 10/9, l = 0.75, \lambda = 4$ in Figure 1. Both potentials could be used to model the biologically motivated interplay between short-range repulsion and long-range attraction, and there is no clear reason to prefer one over the other. A significant difference is the behavior at zero, where Morse is finite and Quasi-Morse is singular though locally integrable for $n > 1$, which are the dimensions we aim to study. The parameter dependence of catastrophic regimes is inherited from the Morse potential:

Corollary 2. *The function $U(r)$ has a unique minimum if and only if $l < 1$, $Cl^{n-2} > 1$. Furthermore, the Quasi-Morse potential $U(|x|)$ is catastrophic if $Cl^n < 1$.*

Proof. Let $U(r) = V(r) - CV\big(\frac{r}{l}\big)$, then $U'(r) = V'(r) - \frac{C}{l}V'\big(\frac{r}{l}\big)$, and the condition for a local extremum can be stated as

$$\frac{C}{l}\,\frac{V'\big(\frac{r}{l}\big)}{V'(r)} = 1.$$

We set $h(r) = \frac{C}{l}\,\frac{V'(\frac{r}{l})}{V'(r)}$, then

$$\begin{aligned} h'(r) &= \frac{C}{l(V'(r))^2}\big(\tfrac{1}{l}V''(\tfrac{r}{l})V'(r) - V'(\tfrac{r}{l})V''(r)\big) \\ &= \frac{C}{l(V'(r))^2}\big(-\tfrac{n-1}{r}V'(r)V'(\tfrac{r}{l}) + \tfrac{1}{l}V(\tfrac{r}{l})V'(r) + \tfrac{n-1}{r}V'(r)V'(\tfrac{r}{l}) \\ &\quad - V(r)V'(\tfrac{r}{l})\big) = \frac{C}{l(V'(r))^2}\big(\tfrac{1}{l}V'(r)V(\tfrac{r}{l}) - V'(\tfrac{r}{l})V(r)\big), \end{aligned}$$

where we used that V is a solution of $\frac{n-1}{r}V'(r) + V''(r) = V(r)$.

We next check that $\log(-V(r))$ is a convex function of r (at least in dimensions $n = 1, 2, 3$). Indeed, if $n = 1$ then $\log(-V(r))$ is affine; if $n = 3$ then $\log(-V(r)) = -\log r - r - \log(4\pi)$. In the case $n = 2$ we have

$$(\log(-V(r)))'' = \frac{K_0(x)^2 + K_2(x)K_0(x) - 2K_1(x)^2}{2K_0(x)^2},$$

and we can use the inequality $K_0(x)^2 + K_2(x)K_0(x) - 2K_1(x)^2 > 0$ (which can be verified numerically).

Thus, if $l < 1$ we have $\frac{V'(\frac{r}{l})}{V(\frac{r}{l})} \geq \frac{V'(r)}{V(r)}$. Since $V(r) < 0$, $V'(r) > 0$, this implies $V'(\frac{r}{l})V(r) - V'(r)V(\frac{r}{l}) \geq 0$, and therefore

$$\begin{aligned} h'(r) &= \frac{C}{l(V'(r))^2}\big(\tfrac{1}{l}V'(r)V(\tfrac{r}{l}) - V'(\tfrac{r}{l})V(r)\big) \\ &< \frac{C}{l(V'(r))^2}\big(V'(r)V(\tfrac{r}{l}) - V'(\tfrac{r}{l})V(r)\big) \leq 0. \end{aligned}$$

Similarly, if $l > 1$ we obtain $h'(r) > 0$.

Further, it is directly checked that $\lim\limits_{r\to 0+} h(r) = Cl^{n-2}$ and $\lim\limits_{r\to\infty} h(r) = 0$ if $l < 1$ and $\lim\limits_{r\to\infty} h(r) = +\infty$ if $l > 1$. Thus, the equation $h(r) = 1$ has no solution in the cases $Cl^{n-2} < 1$, $l < 1$ or $Cl^{n-2} > 1, l > 1$ and a unique positive solution in the cases $Cl^{n-2} < 1$, $l > 1$ or $Cl^{n-2} > 1, l < 1$. Recalling that $U'(r) = V'(r)(1 - h(r))$ we see that of the last two cases, the former corresponds to a local maximum of $U(r)$ and the latter to a local minimum. Finally, by construction we have $\int_{\mathbb{R}^n} V(|x|)\mathrm{d}x = -1\,\forall n$. Therefore, we get

$$\int_{\mathbb{R}^n} U(|x|)\mathrm{d}x = \int_{\mathbb{R}^n} V(|x|) - CV(|x|/l)\mathrm{d}x = -1 + Cl^n,$$

which is negative for $Cl^n < 1$ and thus U is catastrophic (see [38], p. 37).

Remark 1. *Concerning the H-stability of the Quasi-Morse potentials, we remark that the inverse Fourier transform of $U(r)$ for $k = 1$ reads*

$$\check{U}(|\xi|) = \frac{Cl^n - 1 + l^2(Cl^{n-2} - 1)|\xi|^2}{(1 + |\xi|^2)(1 + l^2\,|\xi|^2)}.$$

which is positive if $Cl^n > 1$ and $Cl^{n-2} > 1$. This indicates H-stability, but the criteria developed in [38] do not apply directly, since $\check{U}(|\xi|)$ is not integrable in dimensions $n = 2, 3$. However, our findings presented in the following sections will suggest H-stability for the configurations $l < 1, Cl^{n-2} > 1, Cl^n > 1$. This corresponds to potentials, which posses a unique minimum and a positive $n-$dimensional integral.

Next, we mention the influence of the free scaling parameter k and show that any potential shape can be normalized to $k = 1$. The following results are given without proof which follows easily by a change of variables from the convolution form in radial coordinates (8) and (9) in subsection 2.2.

Corollary 3. *Let ρ be the flock (resp. mill) solution setting $k = 1$ with support $B(0, R)$ (resp. $B(R_m, R_M)$), then the transformed solution $\tilde{\rho}$ for the potential scaled to $k = \tilde{k} \neq 1$ is given by*

$$\begin{cases} \textit{flock:} & \tilde{\rho}(x) = \tilde{k}^n \rho(\tilde{k}x)\,,\ \mathrm{supp}(\tilde{\rho}) = B(0, \frac{R}{\tilde{k}}) \\ \textit{mill:} & \tilde{\rho}(x) = \tilde{k}^2 \rho(\tilde{k}x)\,,\ \mathrm{supp}(\tilde{\rho}) = B(\frac{R_m}{\tilde{k}}, \frac{R_M}{\tilde{k}}) \end{cases}.$$

Denoting $\tilde{U}(r) := U(\tilde{k}r)$, $\tilde{W}(x) = \tilde{U}(|x|)$, we have $\tilde{W} \star \tilde{\rho} = W \star \rho = C\tilde{k}^{2-n}$ for flocks, and $\tilde{W} \star \tilde{\rho} = W \star \rho + \frac{\alpha}{\lambda\beta} \log(\tilde{k})$ for mill solutions.

We conclude the introduction of our potentials with a remark on the corresponding Helmholtz equations, which will be needed later:

Remark 2. *The n-dimensional* Helmholtz equation *reads $\Delta u + k^2 u = 0$ in $\mathbb{R}^n$. Its fundamental system of radially symmetric solutions is associated to a second-order ordinary differential equation (in radial coordinates for $n = 2, 3$) and given below, together with the fundamental system of the already mentioned screened Poisson equations:*

Helmh.	*# 1*	*# 2*
$n = 1$	$\frac{1}{2k}\sin(kr)$	$-\frac{1}{2k}\cos(kr)$
$n = 2$	$-\frac{1}{2\pi}J_0(kr)$	$\frac{1}{2\pi}Y_0(kr)$
$n = 3$	$\frac{1}{4\pi}\frac{\sin(kr)}{r}$	$-\frac{1}{4\pi}\frac{\cos(kr)}{r}$

s.Poiss.	*# 1*	*# 2*
$n = 1$	$\frac{1}{2k}e^{kr}$	$-\frac{1}{2k}e^{-kr}$
$n = 2$	$\frac{1}{2\pi}I_0(kr)$	$-\frac{1}{2\pi}K_0(kr)$
$n = 3$	$\frac{1}{4\pi}\frac{e^{kr}}{r}$	$-\frac{1}{4\pi}\frac{e^{-kr}}{r}$

3.2. Explicit solvability

We start by a simple computation related to the local properties of our potential.

Lemma 1. *Let V be the fundamental solution of the screened Poisson equation. Then*

$$\Delta_x \left(V\left(\frac{x}{l}\right)\right) = \frac{k^2}{l^2} V + l^{n-2}\delta_0.$$

Proof. Let ξ be a test function. Then by change of variables

$$\begin{aligned}\int_{\mathbf{R}^n} \Delta_x \left(V\left(\frac{x}{l}\right)\right) \xi(x)\,\mathrm{d}x &= \frac{1}{l^2}\int_{\mathbf{R}^n} (\Delta V)\left(\frac{x}{l}\right)\xi(x)\mathrm{d}x = \frac{1}{l^2}\int_{\mathbf{R}^n} \Delta V(z)\xi(lz) l^n \mathrm{d}z \\ &= \frac{l^n}{l^2}\left(\int_{\mathbf{R}^n} k^2 V(z)\xi(lz)\mathrm{d}z + \xi(0)\right) \\ &= \frac{1}{l^2}\int_{\mathbf{R}^n} k^2 V(z)\xi(lz) l^n \mathrm{d}z + l^{n-2}\xi(0) \\ &= \frac{k^2}{l^2}\int_{\mathbf{R}^n} V\left(\frac{x}{l}\right)\xi(x)\mathrm{d}x + l^2\xi(0)\end{aligned}$$

leading to the weak formulation of the claim.

Let us now define the operators $\mathcal{L}_1 := \Delta - k^2 I$, $\mathcal{L}_2 := \Delta - \frac{k^2}{l^2} I$ (see Remark 3, [5]) and consider the characteristic equation

$$(W \star \rho)(r) = s(r) \text{ on } \operatorname{supp}(\rho) \tag{10}$$

with some radial $s(r)$ on $\operatorname{supp}(\rho) = B(R_m, R_M)$, $0 \le R_m < R_M$. We apply both operators to the equation and obtain

$$\begin{aligned}\mathcal{L}_2\mathcal{L}_1(W\star\rho) = (\mathcal{L}_2\mathcal{L}_1 W)\star\rho &= \lambda\left(-C\,\mathcal{L}_1\mathcal{L}_2 V\left(\frac{r}{l}\right) + \mathcal{L}_2\mathcal{L}_1 V(r)\right)\star\rho \\ &= \lambda\left(-Cl^{n-2}\Delta\delta + Ck^2 l^{n-2}\delta + \Delta\delta - \frac{k^2}{l^2}\delta\right)\star\rho \\ &= \lambda(1-Cl^{n-2})\Delta\rho + \lambda\left(Ck^2 l^{n-2} - \frac{k^2}{l^2}\right)\rho = \mathcal{L}_2\mathcal{L}_1 s\end{aligned}$$

using Lemma 1. Hence, ρ should satisfy the following equation in its support:

$$\Delta\rho \pm a^2\rho = \frac{1}{\lambda}\frac{1}{1-Cl^{n-2}}\mathcal{L}_2\mathcal{L}_1 s, \tag{11}$$

with $a^2 = |A|$ and

$$A = \frac{Ck^2 l^{n-2} - \frac{k^2}{l^2}}{1-Cl^{n-2}} = k^2\frac{Cl^n - 1}{l^2 - Cl^n},$$

resulting in the Helmholtz equation for $A > 0$, the screened Poisson equation for $A < 0$ and the Poisson equation for $A = 0$. The right-hand side of (11)

is dependent of $s(r)$, and thus on the particular type of solution we wish to compute. For flocks in any dimension and $s(r)$ a constant function, we have $\frac{1}{\lambda(1-Cl^{n-2})}\mathcal{L}_2\mathcal{L}_1 s(r) = \tilde{D}$, also a constant. For mills and $n = 2$ we have $s(r) = D + \frac{\alpha}{\beta}\log(r)$ and obtain

$$\frac{1}{\lambda(1-C)}\mathcal{L}_2\mathcal{L}_1\left[D + \frac{\alpha}{\beta}\log(r)\right] = \frac{k^4}{\lambda l^2(1-C)}\frac{\alpha}{\beta}\log(r) + \tilde{D} \tag{12}$$

since $\log(r)$ is the fundamental solution of the Laplacian and its Dirac delta disappears, since we look for mill solutions on an annulus (see Section 2, (7)). The inhomogeneous solution of (11) for $A \neq 0$ with unknown constant right-hand side $\tilde{D}$ is

$$\rho_{\text{inhom},A}(r) = \frac{\tilde{D}}{A}\,\mathbb{1}_{\text{supp}\,\rho}\,,$$

In the mill case, the inhomogeneous solution of (11) with right-hand side (12) can also be written explicitly. Again since $\log(r)$ is a fundamental solution of the Laplacian and the support of the solution is assumed not to contain the origin, it states

$$\rho_{\text{inhom},A}(r) = \frac{k^4}{\lambda a^2 l^2(1-C)}\frac{\alpha}{\beta}\log(r) + \frac{\tilde{D}}{A} \text{ on } \text{supp}\,\rho \text{ for } A \neq 0.$$

Concerning radially symmetric solutions of the Poisson equation, we have its fundamental solution and the constant as homogenous solutions. The inhomogeneous solution for the flock case is

$$\rho_{\text{inhom},0} = \begin{cases} \frac{1}{4}\tilde{D}r^2 & ,n = 2 \\ \frac{1}{6}\tilde{D}r^2 & ,n = 3 \end{cases},$$

whereas in the mill case it reads

$$\rho_{\text{inhom},0} = \frac{\alpha}{\beta}\frac{k^4}{4\lambda l^2(1-C)}r^2(\log(r) - 1) + \frac{1}{4}\tilde{D}r^2.$$

Together with the radial homogeneous solutions of the Helmholtz, the screened Poisson, and the Poisson equation in Remark 2, we can state the (affine) space to which a solution of (10), if existent, has to be an element of. For flocks, the space of candidate solutions is of lower dimension, since singularities at the origin are excluded. Summarizing, we have:

Corollary 4. *Assume there exists a solution of* $(W \star \rho)(r) = s(r)$ *on* $\text{supp}(\rho)$ *with* W *being the Quasi-Morse potential and* $\text{supp}(\rho) = B(0, R_F)\,, s(r) = D$ *for flocks, or* $\text{supp}(\rho) = B(R_m, R_M)\,, s(r) = D + \frac{\alpha}{\beta}\log(r)$ *for mills respectively. Then* ρ *has to be of the following form on* $\text{supp}\,\rho$ *:*

$n=2$:	*flock*	$A>0$	$\rho_F = \mu_1\, J_0(ar) + \mu_2$
		$A=0$	$\rho_F = \mu_1 r^2 + \mu_2$
		$A<0$	$\rho_F = \mu_1\, I_0(ar) + \mu_2$
	mill	$A>0$	$\rho_M = \rho_{inhom} + \mu_1\, J_0(ar) + \mu_2\, Y_0(ar) + \mu_3$
		$A=0$	$\rho_M = \frac{\alpha}{\beta}\frac{k^4}{4\lambda l^2(1-C)} r^2(\log(r)-1) + \mu_1 r^2 + \mu_2 \log(r) + \mu_3$
		$A<0$	$\rho_M = \rho_{inhom} + \mu_1\, I_0(-ar) + \mu_2 \cdot K_0(ar) + \mu_3$
$n=3$:	*flock*	$A>0$	$\rho_F = \mu_1\, \sin(ar)\frac{1}{r} + \mu_2$
		$A=0$	$\rho_F = \mu_1 r^2 + \mu_2$
		$A<0$	$\rho_F = \mu_1 \sinh(ar)\frac{1}{r} + \mu_2$

with $A = k^2\frac{Cl^n-1}{l^2-Cl^n}$ *,* $a^2 = |A|$*, and* ρ *has to satisfy* $\rho > 0, \int \rho \mathrm{d}x = 1$*.*

The coefficients (μ_1, μ_2) or (μ_1, μ_2, μ_3) have to be computed numerically under the constraint that the solution has to be non-negative, has to contain unit mass, and has to solve the original equation (10), but only on its own support which is a priori unknown. In the next section, we will show an algorithm to solve this problem and present the numerical result.

Remark 3. *We would like to stress that the operators* $\mathcal{L}_1, \mathcal{L}_2$ *have already been used in* [5] *to compute fully explicit stationary solutions of the aggregation equation* $\partial_t \rho + (\rho(\nabla_x W \star \rho))_x = 0$*, equipped with the Morse potential in one dimension. Since stationary flock states of the aggregation equation are traveling wave-like solutions of the velocity dependent model discussed here, the case of one dimension has been treated with even explicit coefficients. The authors arrived at the same operators independently when initially discussing numerical conditioning of equation* (10)*. We mention, that if one wants to solve* (10) *directly, the linear operator matrix, which is usually highly ill-conditioned due to the convolution, becomes well-condition in case of Quasi-Morse potentials.*

4. Numerical investigations

In this section, we show how to numerically determine the support and linear factors μ_i of the stationary flock and mill solution, and present results which are compared to particle simulations.

4.1. The algorithm

Let parameters $n, C, l, k, \alpha, \beta$ be fixed. Let R_{max} be a maximal radius. Our first algorithm determines the best possible solution for *one* particular support $B(R_l, R_r)$. Non-negativity and unit mass of ρ are hard constraints, whereas the deviation $W \star \rho - s$ serves as objective function.

Algorithm 1 (for flocks).

Input : fixed support $B(0, R_r)$, discretization size Δr
- Define radial grid $\bar{r} = \{r_0, \dots, r_N\}$ s.t. $r_0 = 0, r_N = R_r, r_{i+1} - r_i = \Delta r \, \forall i$.
- Denote $\bar{\rho}$ the approximation of ρ on $\bar{r}$ (likewise for other functions).
- Compute a matrix H s.t. $\overline{W \star \rho} = H\bar{\rho}$ according to Section 2.2.
- Evaluate ρ_{hom} and 1 on $\operatorname{supp}\rho$. Convolve $g^1 := H\bar{\rho}_{\text{hom}}, g^2 := H\,\bar{1}$.
- Solve $\mu_{\text{const}} := \begin{pmatrix} g_1^1 & g_1^2 \\ g_N^1 & g_N^2 \end{pmatrix} \backslash \begin{pmatrix} 1 \\ 1 \end{pmatrix}$ (which means setting $D = 1$ temporarily).
- Set $\bar{\rho} := \frac{1}{M}(\mu_{\text{const},1}\rho_{\text{hom}} + \mu_{\text{const},2})$ with M normalizing total mass.
- Measure deviation from arbitrary constant as

$$e := \frac{1}{R_r} \int \left[H\bar{\rho} - \frac{1}{R_r} \int H\bar{\rho} \mathrm{d}\bar{r} \right] \mathrm{d}\bar{r}.$$

Output : $e, \bar{\rho}, \bar{s}$ if $\bar{\rho} \geq 0$

Here, ρ_{hom} denotes the homogeneous solution dependent on dimension as in Corollary 4. For the case of mills, we have to take the fixed inhomogeneous solution into account:

Algorithm 1 (for mills).

Input : fixed support $B(R_m, R_M)$, discretization size Δr
- Define radial grid $\bar{r} = \{r_0, \dots, r_N\}$ s.t. $r_0 = r_l, r_N = R_r, r_{i+1} - r_i = \Delta r \, \forall i$.
- Denote $\bar{\rho}$ the approximation of ρ on $\bar{r}$ (likewise for other functions).
- Compute a matrix H s.t. $\overline{W \star \rho} = H\bar{\rho}$ according to Section 2.2.
- Evaluate $\rho_{\text{inhom},A}$ on $\operatorname{supp}\rho$ and convolve $\bar{s}_{\text{inhom}} := H\bar{\rho}_{\text{inhom},A}$.
- Define $\bar{s}_{\text{rem}} := \bar{s} - \bar{s}_{\text{inhom}}$.
- Evaluate $J_0(ar), Y_0(ar)$ and 1 on $\operatorname{supp}\rho$.
  Convolve $g^1 := H\bar{J}_0, g^2 := H\bar{Y}_0, g^3 := H\bar{1}$.
- Solve $\mu_{\text{rem}} := \begin{pmatrix} g_1^1 & g_1^2 & g_1^3 \\ g_j^1 & g_j^2 & g_j^3 \\ g_N^1 & g_N^2 & g_N^3 \end{pmatrix} \backslash \begin{pmatrix} \bar{s}_{\text{rem},1} \\ \bar{s}_{\text{rem},j} \\ \bar{s}_{\text{rem},N} \end{pmatrix}$ with $j := \lfloor N/2 \rfloor$.
- Solve $\mu_{\text{const}} := \begin{pmatrix} g_1^1 & g_1^2 & g_1^3 \\ g_j^1 & g_j^2 & g_j^3 \\ g_N^1 & g_N^2 & g_N^3 \end{pmatrix} \backslash \begin{pmatrix} 1 \\ 1 \\ 1 \end{pmatrix}$ (setting $D = 1$ temporarily).
- Set $\bar{\rho}_{\text{rem}} := \mu_{\text{rem},1}\bar{J}_0 + \mu_{\text{rem},2}\bar{Y}_0 + \mu_{\text{rem},3}$ and
  $\bar{\rho}_{\text{const}} := \mu_{\text{const},1}\bar{J}_0 + \mu_{\text{const},2}\bar{Y}_0 + \mu_{\text{const},3}$.
- Set $\bar{\rho} := \bar{\rho}_{\text{inhom},A} + \bar{\rho}_{\text{rem}} + \gamma\bar{\rho}_{\text{const}}$ with $\gamma := \frac{1 - m(\bar{\rho}_{\text{rem}}) - m(\bar{\rho}_{\text{inhom},A})}{m(\bar{\rho}_{\text{const}})}$.
- Measure deviation

$$e_1 := \frac{1}{R_M - R_m} \int \left[H\bar{\rho} - \bar{s} - \frac{1}{R_M - R_m} \int (H\bar{\rho} - \bar{s}) \mathrm{d}\bar{r} \right] \mathrm{d}\bar{r}.$$

- Penalize convexity of $\bar{s}$ by $e_2 := \int \chi_{[\bar{s}'' > 0]}\, \bar{s} \mathrm{d}\bar{r}$

Output : $e = e_1 + e_2, \bar{\rho}, \bar{s}$ if $\bar{\rho} \geq 0$

Now, we search the minimizer of the error function e over a test set of supports, given by a pre-defined discretization Δr and maximal support size

$R_{\max}$. Repeating Algorithm 1 over the set of test supports provides a minimizer. For flocks, the number of tested supports is $\approx \frac{R_{\max}}{\Delta r}$, for mills $\approx \frac{1}{2}\left(\frac{R_{\max}}{\Delta r}\right)^2$. To enhance the speed of numerical computation, we first compute a solution based on a coarse discretization length Δr_1. Then, the obtained minimizer is used as the center of a local refinement search with a fine discretization length, as illustrated in Algorithm 2:

Algorithm 2.

- Choose a coarse grid length Δr_1 such that an iteration of Algorithm 1 over all test supports is reasonably fast.
- Vary the obtained support $B(0, R_{F,1})$ ($B(R_{m,1}, R_{M,1})$) up to a constant c.
- Choose $\Delta r_2 \ll \Delta r_1$ and re-run Algorithm 1 restricted on $|R_F - R_{F,1}| \leq c$ ($|R_m - R_{m,1}| \leq c, |R_M - R_{M,1}| \leq c$ for mills).

Naturally, the matrix H is not recomputed in every iteration but constructed once for the largest support and inherited. The choice to fix a functional equality on the points which are most left, most right and for mills central on the chosen support is arbitrary. We say that no compact solutions are found in our computations, if our algorithms deliver $R_{\max}$ as the error minimizer, no matter of its value. The convergence of the algorithm for $\Delta r \to 0$ if compact solutions are found will be demonstrated together with the results of the next subsection.

4.2. Flocks in 2D

We start our presentation of numerical results with the aligned flock in two dimensions. Our standard example is the configuration $C = \frac{10}{9}, l = 0.75, k = \frac{1}{2}$ as in Fig. 1. The stationary aligned flock state is independent of λ, α, β, yet emergence of flocks in particle simulations depends on these parameters and suitable initial conditions. An exemplary convenient choice is $\alpha = 1, \beta = 5, \lambda \in \{100, 1000\}$. The observed flock of aligned particles is illustrated in Fig 2a for $N = 400$ particles. In Fig. 2b, the result of our investigations is compared to the empirical radial density obtained from a particle simulation with $N = 16000$ agents. We see that the continuous solution matches the particle density and convergence is expected as $N \to \infty$. While the numerical cost of full particle simulations is at least $\mathcal{O}(N^2)$, the computational effort of the presented method scales quadratically with Δr, as illustrated in Fig. 3b. In Fig. 3a we show the convergence of our algorithms as $\Delta r \to 0$. One observes that the support is estimated well for coarse grid sizes, whereas the correct radial density is established with finer discretizations. The minimal error values of Algorithms 1,2 are listed in Fig. 3b. The advantages of the presented solution are continuity, dramatic reduction of the numerical cost, fast convergence, and an explicit expression of the radial density as, in this example, a combination of Bessel's J-function and a constant.

Concerning the potential parameters, the area of relevant short-term repulsion and long-range attraction shapes divides into two subregion based on the results of section 3, as illustrated in Fig. 4: In region I with $C > 1, l < 1, Cl^2 < 1$,

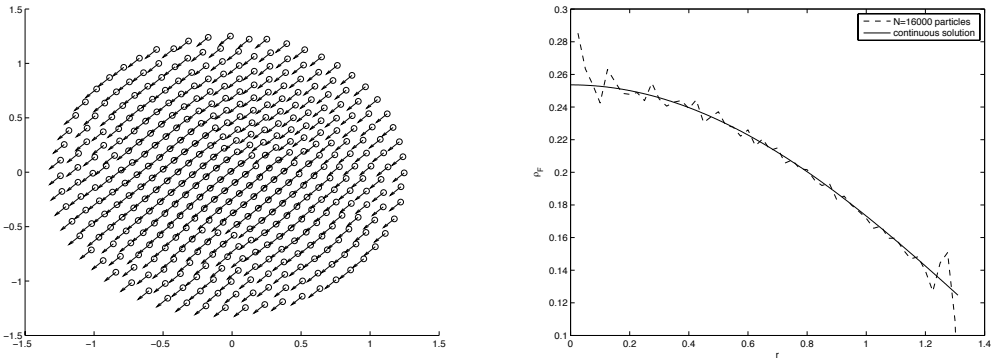

(a) Flock emerged in a particle simulation with $N = 400$ particles

(b) Radial flock density: Continuous result vs. empirical density ($N = 16000$ particles)

Figure 2: Two-dimensional aligned flocks emerge for the Quasi-Morse potential. The resulting continuous radial density of Algorithms 1,2 matches the empirical distribution obtained from particle simulations. The stationary flock has the form $\rho_F = \mu_1 J_0(ar) + \mu_2$ with, in this case, $\mu_1 \approx 0.2356, \mu_2 \approx 0.018, A = 1.5, R_F \approx 1.31$ (Quasi-Morse potential parameters in use are $C = \frac{10}{9}, l = 0.75, k = \frac{1}{2}$).

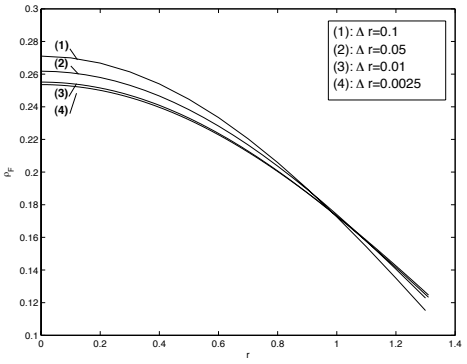

(a) Continuous solution ρ_F for varying Δr

Δr	error e	computation time
0.1	3.54e-05	0.76s
0.05	1.36e-05	2.85s
0.01	3.99e-06	69.1s
0.0025	9.97e-07	1125s

(b) Minimal error value and computation times

Figure 3: Algorithms 1,2 converge as $\Delta r \to 0$ if a compactly supported flock solution exists. Four resulting densities are shown for $\Delta r \in \{0.1, 0.05, 0.01, 0.0025\}$ together with the minimal error value of the algorithm and the corresponding computation time.

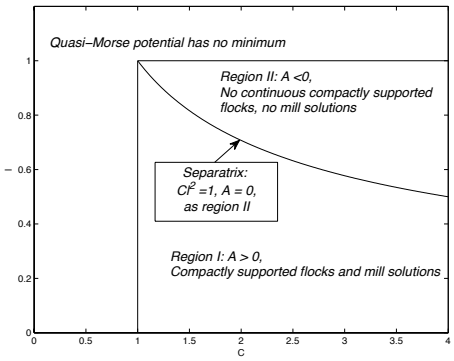

Figure 4: Phase diagram of the Quasi-Morse potential in 2D: The biologically relevant scenarios decompose into two subregion. Region I: $A > 0$, continuous compactly supported flocks. Region II: $A \leq 0$, no compactly supported continuous solutions, flocks only emerge on particle level. The same division of regions applies to the mill solutions.

the potential is catastrophic, $A > 0$ and compactly supported continuous flock solutions are found. In region II with $C > 1, l < 1, Cl^2 < 1, A < 0$, no compactly supported solutions can be found, which indicates H-stability. Flocks in particle simulations emerge, but do not approach a compact support as $N \to \infty$. The presented method faces numerical difficulties for catastrophic potentials with $Cl^2 \approx 1$, where it eventually breaks down. Similarly, particle simulation are not fully reliable in this limiting case. However, thanks to our computation in Section 3 we are able to consider the separatrix case $Cl^2 = 1, C > 1, l < 1, A = 0$: Here, no compact solutions are found. Our findings are illustrated in Fig. 4.

4.3. Mills in 2D

The Quasi-Morse potential is able to produce rotating mill states in particle simulations, just as the original Morse potential. We choose the same configuration as in Section 4.2 with $\lambda = 100$ and show the mill emerging from a particle simulation in Figure 5a. The resulting mill solution of our algorithms is illustrated in Figure 2b, together with a comparison to a empirical density from a particle mill with $N = 16000$ agents. Again, our result is confirmed by the particle simulation and support as well as density shape agree perfectly. The stationary rotating mill is a weighted sum of Bessel's J and Y functions, the inhomogenity ρ_{hom} and a constant. The convergence of Algorithms 1, 2 in the mill case is shown in Figure 6. As for flocks, the computational costs are minimal compared to a full particle simulation. For the existence of compactly supported mill solutions, the parameter diagram on Figure 4 applies just as for flocks. In region I, continuous solutions can be found, whereas in region II and the separatrix $Cl^2 = 1$ no such mills can be found. In particle simulations, we there see either a crystal-like arrangements or "finite particle" flocks as in Section 4.2. Next we study the impact of parameters α, β, λ on the stationary

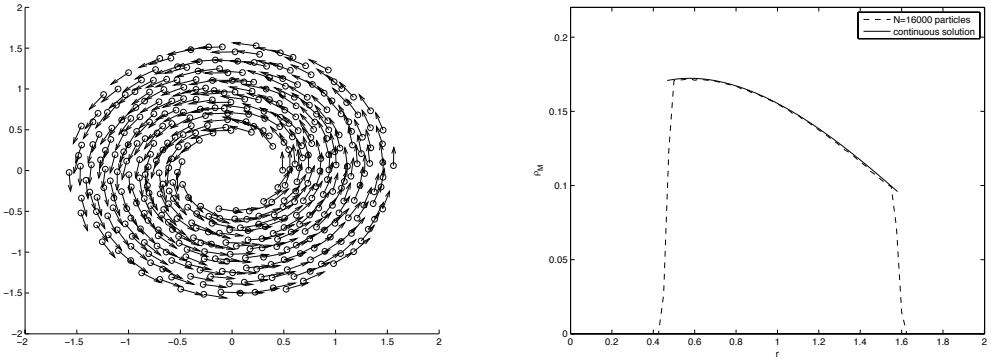

(a) Mill emerged in a particle simulation with $N = 400$ particles

(b) Radial mill density: Continuous result vs. empirical measure ($N = 16000$ particles)

Figure 5: Rotating mills emerge for the Quasi-Morse potential. As for flocks, the resulting radial density of Algorithms 1,2 matches the empirical distribution obtained from particle simulations. The mill solution has the form $\rho_M = \rho_{\text{inhom},A} + \mu_1\, J_0(ar) + \mu_2\, Y_0(ar) + \mu_3$ with, in this case, $\mu_1 \approx 0.1708, \mu_2 \approx 0.0468, \mu_3 = 0.0320, A = 1.5, \text{supp}_{\rho_M} \approx B(0.47, 1.57)$ (Quasi-Morse potential parameters in use are $C = \frac{10}{9}, l = 0.75, k = \frac{1}{2}$, others are $\alpha = 1, \beta = 5, \lambda = 100$).

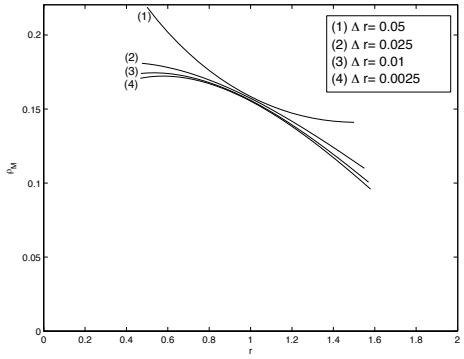

Figure 6: Algorithms 1,2 converge for the mill case as $\Delta r \to 0$.

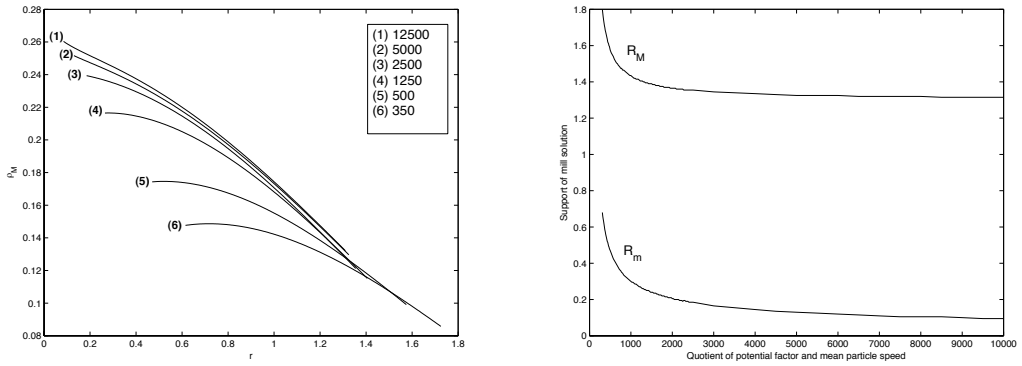

(a) mill solutions for varying $\frac{\beta\lambda}{\alpha}$ (b) support of mill solutions for varying $\frac{\beta\lambda}{\alpha}$

Figure 7: Quasi-Morse potentials with identical shape parameters C, l, k result in mill solutions with different support sizes and densities, depending on the ratio of potential factor and squared stationary speed of the mill.

mill solution, which enter the solution solely in the joint quotient $\frac{\alpha}{\lambda\beta}$. Hence, for a potential multiplied by a factor λ, the mill solution will stay the same, if the preferred speed of particles is multiplied by $\sqrt{\lambda}$ by any suitable change of α and/or β. In Figure 7a, we show several mill densities for our standard potential configuration and $\frac{\beta}{\lambda\,\alpha} \in \{350, 500, 1250, 2500, 5000, 12500\}$. The support of mill solutions is plotted against $\frac{\beta}{\lambda\,\alpha}$ in Figure 7b.

4.4. Flocks in 3D

The introduction of Quasi-Morse potentials enables us also to study flocks in three space dimensions. As we have mentioned in Section 3, the area of admissible parameter configurations is smaller than in the 2D case, as illustrated in the parameter diagram For our example, we set $C = 1.255, l = 0.8, k = 0.2, A = 5.585$ and plot the resulting potential shape in Figure 8a. A three-dimensional flock resulting from a particle simulation is shown in Figure 8b. With the help of Algorithms 1,2 the continuous radial flock density is computed as a linear combination of $\frac{\sin ar}{r}$ and a constant. Also in three dimensions, the empirical density of a particle simulation matches our result, as illustrated in Figure 8c. Concerning the existence of flock solutions in dependence of the shape parameters C and l, we get an equivalent picture as in two dimensions (see Figure 8d): Though different in shape, the area of biologically relevant shapes is divided into two subregions by the separatrix $Cl^3 = 1$. In region I, continuous compactly supported three-dimensional flocks are found, not so in region II, which again indicates H-stability. Here, flocks do appear but their support increases with the total number of agents N. In the special case of the separatrix, which can be investigated with the computation of the case $A = 0$ in Section 3, no flock solutions are found.

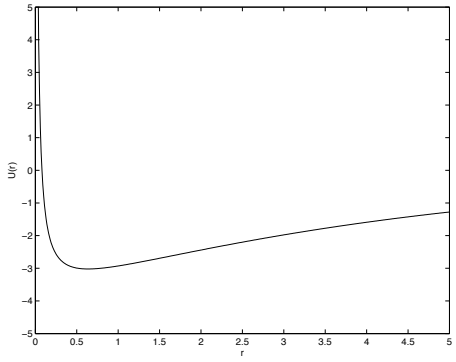

(a) Quasi-Morse potential in 3D

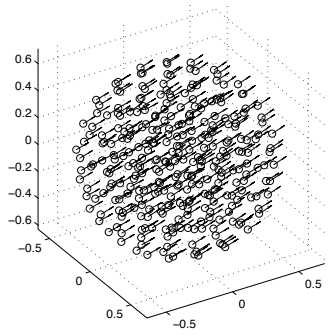

(b) 3D flock emerged in a particle simulation with $N = 200$ particles

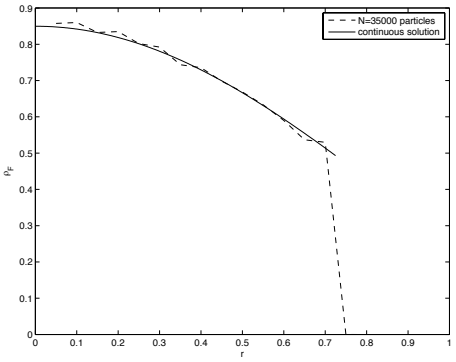

(c) 3D radial flock density: continuous result vs. empirical measure ($N = 35000$ particles)

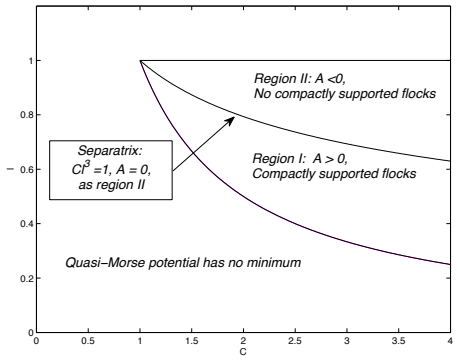

(d) Parameter diagram

Figure 8: The Quasi-Morse potential in three dimension is able to produce aligned flock solutions. The continuous radial density can be expressed as $\rho_F = \mu_1 \cdot \sin(ar)\frac{1}{r} + \mu_2 \cdot 1$ with, in this case, $\mu_1 \approx 0.3574, \mu_2 \approx 0.0052, R_F \approx 0.725, A = 5.585$. Our result is verified by comparing to the empirical density obtained from a particle simulation. (a) Exemplary potential shape, (b) Flock emerged from 3D particle simulation, (c) Continuous flock solution vs empirical measure, (d) Parameter diagram of biological relevant configurations

5. Discussion

Quasi-Morse potentials fulfill three properties desirable from biological modeling: short-term repulsion, long-term attraction and vanishing interaction at infinity. Using Quasi-Morse potentials instead of the standard Morse potential makes, in our view, hardly any difference in terms of biological modeling. The stronger singularity at the origin for $n \neq 2$ might even be desirable in order to enforce repulsion. Though the special functions involved for $n = 2$ may seem not as convenient to work with as the exponential function, existence of continuous, compactly supported stationary states itself make Quasi-Morse potentials a good choice for further studies of the models discussed in the above. Our results are, to the best of our knowledge, one of the first of its kind for explicit solutions of flock and mill patterns in two or three dimensions. The strategy of building up potentials from solutions of certain partial differential equations might work in other cases as well and form one tool in the effort to understand equilibria of interaction potentials. However, the techniques applied here are of no help for general potentials, such as classical Morse. With a variety of potentials suggested (see the discussion in Section 2), the problem of choosing the best suited one for a particular biological application becomes increasingly evident and should be a topic of future research.

6. Conclusions

In this paper we have introduced the Quasi-Morse interaction potentials for a second-order model of self-propelled interactive particles. The Quasi-Morse potentials lead to the emergence of flocks and mills, similar to the standard Morse potential. We have shown, that the radial densities of these stationary states are (affine) linear combinations of two or three elementary functions, which are chosen with the respect to the three subcases $A > 0$ (catastrophic), $A = 0$ (separatrix) or $A < 0$. In order to determine the correct scalar coefficients and the a priori unknown support, we have developed a numerical algorithm that does not use time evolutions in Section 4. We have illustrated our result with examples for flocks and mills in two dimension and flocks in 3D. In all cases, our findings are convincingly verified by corresponding particle simulations. With our algorithm, we find that for all coherent patterns, only the catastrophic scenarios $A > 0$ lead to continuous compactly supported solutions.

7. Acknowledgements

JAC acknowledges support from the project MTM2011-27739-C04-02 DGI-MICINN (Spain) and 2009-SGR-345 from AGAUR-Generalitat de Catalunya. We also acknowledge the Isaac Newton Institute for the Mathematical Sciences, where part of this work was accomplished.

References

[1] Balagué, D., Carrillo, J.A., Laurent, T., Raoul, G.: *Nonlocal interactions by repulsive-attractive potentials: radial ins/stability*. Preprint UAB.

[2] Ballerini, M., Cabibbo, N., Candelier, R., Cavagna, A., Cisbani, E., Giardina, L., Lecomte, L., Orlandi, A., Parisi, G., Procaccini, A., Viale, M., Zdravkovic, V.: *Interaction ruling animal collective behavior depends on topological rather than metric distance: evidence from a field study*. Proc Natl Acad Sci USA, **105** (2008) , pp. 1232-1237.

[3] Barbaro, A., Taylor, K., Trethewey, P.F., Youseff, L., Birnir, B.: *Discrete and continuous models of the dynamics of pelagic fish: application to the capelin*. Mathematics and Computers in Simulation, **79** (2009), pp. 3397–3414.

[4] Barbaro, A., Einarsson, B., Birnir, B., Sigurthsson, S., Valdimarsson, H., Palsson, O.K., Sveinbjornsson, S., Sigurthsson, T.: *Modelling and simulations of the migration of pelagic fish*. ICES J. Mar. Sci., **66** (2009), pp. 826–838.

[5] A. Bernoff and C. Topaz, A primer of swarm equilibria, *preprint*.

[6] Bolley, F., Cañizo, J.A., Carrillo, J.A.: *Stochastic Mean-Field Limit: Non-Lipschitz Forces & Swarming*. To appear in Math. Mod. Meth. Appl. Sci.

[7] Bonabeau, E., Dorigo, M., Theraulaz, G.: *Swarm Intelligence: From Natural to Artificial Systems*. Intelligence: From Natural to Artificial Systems (Oxford University Press, New York, 1999);

[8] Braun, W., Hepp, K.: *The Vlasov Dynamics and Its Fluctuations in the 1/N Limit of Interacting Classical Particles*. Commun. Math. Phys., **56** (1977), pp. 101-113

[9] Camazine, S., Deneubourg, J.-L., Franks, N.R., Sneyd, J., Theraulaz, G., Bonabeau, E.: Self-Organization in Biological Systems. Princeton University Press (2003)

[10] Cañizo, J.A., Carrillo, J.A., Rosado, J.: *A well-posedness theory in measures for some kinetic models of collective motion*. Math. Mod. Meth. Appl. Sci. **21** (2011), pp. 515-539.

[11] Cañizo, J.A., Carrillo, J.A., Rosado, J.: *Collective Behavior of Animals: Swarming and Complex Patterns*. Arbor **186** (2010), pp. 1035-1049.

[12] Carrillo, J.A., D'Orsogna, M.R., Panferov, V.: *Double milling in self-propelled swarms from kinetic theory*. Kinetic and Related Models, **2** (2009), pp. 363-378.

[13] Carrillo, J.A., Fornasier, M., Toscani, G., Vecil, F., *Particle, Kinetic, and Hydrodynamic Models of Swarming*. Mathematical Modeling of Collective Behavior in Socio-Economic and Life Sciences, Series: Modelling and Simulation in Science and Technology, Birkhauser (2010), pp. 297-336.

[14] Carrillo, J.A., Klar, A., Martin, S., Tiwari, S.: *Self-propelled interacting particle systems with roosting force*. **Math. Mod. Meth. Appl. Sci 20**, (2010), 1533–1552.

[15] Chuang, Y.L., Huang, Y.R., D'Orsogna, M.R., Bertozzi, A.L.: *Multi-vehicle flocking: scalability of cooperative control algorithms using pairwise potentials*. IEEE International Conference on Robotics and Automation (2007), pp. 2292–2299.

[16] Chuang, Y.L., D'Orsogna, M.R., Marthaler, D., Bertozzi, A.L., Chayes, L.: *State transitions and the continuum limit for a 2D interacting, self-propelled particle system*. Physica D, **232** (2007), pp. 33-47.

[17] Couzin, I.D., Krause, J., Franks, N.R., Levin, S.A.: *Effective leadership and decision making in animal groups on the move*. Nature, **433** (2005), pp. 513-516.

[18] Couzin, I.D., Krause, J., James, R., Ruxton, G. and Franks, N.: *Collective memory and spatial sorting in animal groups*. Journal of Theoretical Biology, **218** (2002), pp. 1-11.

[19] Degond, P., Motsch, S.: *Continuum limit of self-driven particles with orientation interaction*. Math. Models Methods Appl. Sci., **18** (2008), pp. 1193-1215.

[20] Dobrushin, R.: *Vlasov equations*. Funct. Anal. Appl., **13** (1979), pp. 115-123.

[21] D'Orsogna, M.R., Chuang, Y.L., Bertozzi, A.L., Chayes, L.: *Self-propelled particles with soft-core interactions: patterns, stability, and collapse*. Phys. Rev. Lett., **96** (2006), 104302

[22] K. Fellner and G. Raoul. Stable stationary states of non-local interaction equations. *Math. Models Methods Appl. Sci.*, **20** (2010), pp. 2267–2291.

[23] K. Fellner and G. Raoul. Stability of stationary states of non-local interaction equations. *Mathematical and Computer Modelling*, **53** (2011), pp. 1436–1450.

[24] R. C. Fetecau, Y. Huang, and T. Kolokolnikov. Swarm dynamics and equilibria for a nonlocal aggregation model. *to appear in Nonlinearity*, 2011.

[25] Grégoire, G., Chaté, H.: *Onset of collective and cohesive motion*. Phy. Rev. Lett., **92** (2004), 025702

[26] E. Hackett-Jones, K. Landman, K. Fellner. Aggregation patterns from non-local interactions: discrete stochatic and continuum modelling, *preprint.*

[27] M. Hauray, P.-E. Jabin, Particles approximations of Vlasov equations with singular forces: Part 2, Preprint.

[28] Hemelrijk, C.K. and Kunz, H.: *Density distribution and size sorting in fish schools*: an individual-based model. Behavioral Ecology, **16** (2005), pp. 178-187.

[29] Hildenbrandt, H, Carere, C., and Hemelrijk, C. K.: *Self-organised complex aerial displays of thousands of starlings: a model.* Preprint, `arXiv:0908.2677` (2009).

[30] Huth, A. and Wissel, C.: *The Simulation of the Movement of Fish Schools.* Journal of Theoretical Biology, **152** (1992), pp. 365-385

[31] Kunz, H. and Hemelrijk, C. K.: *Artificial fish schools: collective effects of school size, body size, and body form.* Artificial Life, **3** (2003), pp. 237-253.

[32] Levine, H., Rappel, W.J., Cohen, I.: *Self-organization in systems of self-propelled particles.* Phys. Rev. E, **63** (2000), 017101.

[33] Li, Y.X., Lukeman, R., Edelstein-Keshet, L.: *Minimal mechanisms for school formation in self-propelled particles.* Physica D, **237** (2008), pp. 699-720.

[34] Li, Y.X., Lukeman, R., Edelstein-Keshet, L.: *A conceptual model for milling formations in biological aggregates.* Bull Math Biol., **71** (2008), pp. 352-382.

[35] Mogilner, A., Edelstein-Keshet, L., Bent, L., Spiros, A.: *Mutual interactions, potentials, and individual distance in a social aggregation.* J. Math. Biol., **47** (2003), pp. 353-389.

[36] Neunzert, H.: *The Vlasov equation as a limit of Hamiltonian classical mechanical systems of interacting particles.* Trans. Fluid Dynamics, **18** (1977), pp. 663-678.

[37] Parrish, J., Edelstein-Keshet, L.: *Complexity, pattern, and evolutionary trade-offs in animal aggregation.* Science, **294** (1999), pp. 99-101.

[38] Ruelle, D.: Statistical mechanics: Rigorous results. W. A. Benjamin, Inc., New York-Amsterdam 1969.

[39] Spohn, H.: *Large scale dynamics of interacting particles.* Texts and Monographs in Physics, Springer (1991).

[40] Vicsek, T., Czirok, A., Ben-Jacob, E., Cohen, I., Shochet, O.: *Novel type of phase transition in a system of self-driven particles*, Phys. Rev. Lett., **75** (1995), pp. 1226-1229.